Formation and Properties of Model Crystalline Blends Comprising Diacetylene-Containing Polyester and Polyolefin: Processing, Thermal Behavior, and Morphology

P. A. Lovell, J. L. Stanford,* Y.-F. Wang, and R. J. Young

Polymer Science and Technology Group, Manchester Materials Science Centre, University of Manchester and UMIST, Grosvenor St, Manchester M1 7HS, U.K.

Received January 22, 1997; Revised Manuscript Received August 27, 1997

ABSTRACT: A series of blends of a specially-synthesized, diacetylene-containing polyester (PE) and a commercial poly[ethylene-*co*-(vinyl acetate)] (EVA) have been prepared by mixing in solution followed by coprecipitation. DSC and WAXD characterization of the two components and each of the blends, before and after compression molding at 120 °C under vacuum, showed that solid-state topochemical cross-polymerization of PE takes place during molding to give polydiacetylene cross-links in PE phases. WAXD also showed that the crystal structures of PE and EVA were unaffected by molding, although composition-dependent reductions in the degrees of crystallinity were evident. The morphologies of molded specimens were examined by using DMA and SEM, together with solvent extraction experiments: blends comprising 20, 40, and 80 wt % PE have continuous−discontinuous morphologies, whereas the blend comprising 60 wt % PE has a cocontinuous morphology. The use of Raman spectroscopy to study deformation in the cross-polymerized PE phase of the blends independent of overall blend deformation is described in the following paper (*Macromolecules*, following paper in this issue).

Introduction

The mechanical properties of immiscible polymer blends are strongly infuenced by morphology and stress transfer between phases.[1−3] Although it is possible to study morphology using a range of established techniques, such as optical and electron microscopy and thermal anaysis, it is much more difficult to probe stress transfer. The present paper is one in a series which describes the preparation of model polymer blends and their use in monitoring deformation micromechanics using Raman spectroscopy. The model blends contain as one component a polydiacetylene-containing phase, the deformation of which can be followed quantitatively by the shift in wavenumber of the polydiacetylene Raman C≡C stretching band. In this way, stress transfer between the polydiacetylene-containing phase and another phase can be monitored across the complete range of blend compositions and morphologies. Although a similar approach has been applied to the study of deformation micromechanics in multiphase copolyurethane systems,[4−7] the morphology of these materials was created *in situ* by phase separation during copolymerization. The present series of papers,[8−11] however, is the first to describe the use of the approach to study deformation micromechanics in polymer blends.

The current paper describes the preparation, morphology, and thermal properties of model polymer blends formed from a diacetylene-containing polyester and a polyolefin. Synthesis and characterization of the diacetylene-containing polyester have already been reported,[10] and a subsequent paper[11] reports mechanical properties and studies of the deformation micromechanics of the model blends using Raman spectroscopy.

Experimental Section

Materials. Diacetylene-containing polyesters of general structure **I** have been prepared by reaction of terephthaloyl chloride with hexane-2,4-diyne-1,6-diol employing benzoyl chloride for control of molar mass. The particular diacetylene-

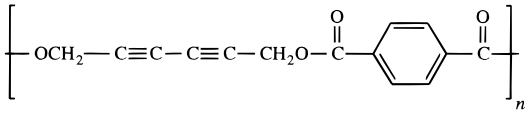

(I)

containing polyester used in this work is that defined as PE4 in an earlier paper[10] which gives details of its preparation and properties. It has a melting temperature of 119 ± 2 °C, a number-average molar mass M_n of 1260 g mol^{-1}, a weight-average molar mass M_w of 1900 g mol^{-1}, and $M_n/M_w \sim 1.5$. In the present and subsequent paper[11] this polyester is more simply designated PE. The poly[ethylene-*co*-(vinyl acetate)], EVA, used is a noncommercial grade, coded UL00206, which was specially supplied by Exxon Chemical (Brussels); the only characterization data provided by Exxon Chemical was the vinyl acetate content, which is nominally 6.5% by weight.

PE4 and EVA charcterisation data of importance to the work described in this paper are presented within the Results and Discussion section.

Processing. Four blends of PE with EVA were prepared by mixing in solution and coprecipitation. The blends are defined by B-20PE, B-40PE, B-60PE, and B-80PE where the numbers in the codes represent the percentage by weight of PE in the blend. PE, EVA, and the dried blends each were molded under vacuum to form specimens for mechanical testing. Details of the procedures used for blending and molding follow.

Solution blending involved dissolution of the required quantities of PE and EVA in a 50:50 (v/v) tetrahydrofuran: toluene mixture at 80 °C and then coprecipitation by addition to a large excess of 20:80 (v/v) methanol:water mixture which was at room temperature. The resulting blends, in the form of cream-colored powders, were dried to constant weight under vacuum in the dark at room temperature.

Molding was carried out using a purpose-designed molding apparatus[12] which enables beams (70 × 10 × 3 mm) to be compression-molded under nitrogen or in *vacuo* at controlled temperature. The apparatus comprises a leaky mold, housed

* To whom correspondence should be addressed.

S0024-9297(97)00071-5 CCC: $15.00
Published on Web 01/22/1998

Table 1. DSC Data for EVA, the Diacetylene-Containing Polyester, PE, and EVA/PE Blends

	T_m/°C[a]		ΔH_m^B/J g^{-1} [b]		ΔH_m^{EVA}/J g^{-1} [c]		T_{cp}^{peak}/°C[d]		ΔH_{cp}^B/J g^{-1} [e]		ΔH_{cp}^{PE}/J g^{-1} [f]	
material	bm[g]	am[g]	bm	am	bm	am	bm	am	bm	am	bm	am
EVA	107	106			75	73						
PE[h]							186[i]	195[i]			574[i]	102[i]
B-20PE	100	102	63	60	79	75	175		89		444	
B-40PE	100	102	47	36	79	60	177		192		480	
B-60PE	100	102	30	16	74	41	179		320		533	
B-80PE	100	102	15	5	75	27	179		442		552	

[a] T_m is the melting temperature of EVA. [b] ΔH_m^B is the enthalpy of fusion of EVA per unit mass of the blend. [c] ΔH_m^{EVA} is the enthalpy of fusion of EVA normalized to EVA content. [d] T_{cp}^{peak} is the peak temperature for cross-polymerization of diacetylene groups. [e] ΔH_{cp}^B is the enthalpy of cross-polymerization of diacetylene groups per unit mass of the blend. [f] ΔH_{cp}^{PE} is the enthalpy of cross-polymerization of diacetylene groups normalized to PE content. [g] bm = before molding; am = after molding. [h] Data for PE as prepared: $T_{cp}^{peak} = 205$ °C, $\Delta H_{cp}^{PE} = 652$ J g^{-1} (see data for PE4 in Table 3 of ref 10). [i] After reprecipitation from 50:50 tetrahydrafuran:toluene.

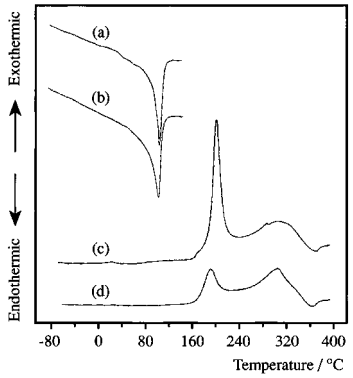

Figure 1. DSC traces of EVA (a) before and (b) after molding and of PE (c) as prepared and (d) after molding. For each pair of traces the sensitivity is constant. (The sensitivity for the EVA traces is approximately 8× greater than for the PE traces.) The traces for EVA show the melting endotherm at 107 °C. The trace for PE as prepared shows the cross-polymerization exotherm with maximum at 205 °C; after molding, however, the exotherm is much weaker indicating that cross-polymerization has taken place.

Scheme 1. Cross-Polymerization of the Diacetylene-Containing Polyester, PE

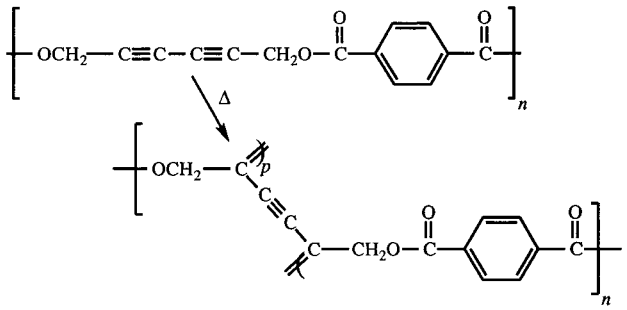

in a heated chamber which can either be filled with an inert gas or be evacuated. Compression of the material is achieved by application of force to the upper, male section of the mold via a screw-driven device fitted through the top of the heated chamber. The mold was filled with an excess of material (approximately 3.5−4.0 g) and placed in the chamber at room temperature. The chamber then was placed in an oven thermostated at 120 °C, evacuated, and left for 3 h to equilibrate. The temperature of the mold was monitored by using a thermocouple attached to the surface of the male section. Following equilibration, compression was applied and maintained at 120 °C for 6 h, by driving the faces of the two sections of the mold into contact. At the end of this period the chamber was moved from the oven and left to cool to room temperature. The moldings produced from the blends showed the deep purple color characteristic of the polydiacetylene cross-links in molded PE.

Characterization. Differential scanning calorimetry, DSC, was performed on a Du Pont 2000 thermal analyst instrument with a DuPont 910 cell base equipped with a DSC cell. Powdered samples (∼10 mg) were analyzed against glass beads (∼10 mg) over the range −80 to 400 °C at a heating rate of 20 °C min^{-1} under nitrogen flowing at 20 mL min^{-1}. Calibrations for temperature and enthalpy change were carried out by using indium.

Dynamic mechanical analysis, DMA, was performed on a Du Pont 983 dynamic mechanical analyzer controlled with a Du Pont 2000 thermal analyst console. Specimens in the form of rectangular beams (40 × 10 × 3 mm) were analyzed in the temperature range −140 to 400 °C at a heating rate of 5 °C min^{-1} using a fixed frequency of 1 Hz and a fixed deformation amplitude of 0.3 mm of the oscillating clamping system. For each material, mean DMA curves of storage modulus, loss modulus, and loss tangent against temperature were derived from separate analyses of four specimens. The instrument was calibrated to account for instrument losses and end-corrections of specimen length.[12]

Wide-angle X-ray diffraction, WAXD, measurements were carried out on a Phillips PW1710 diffractometer equipped with a graphite monochromator and using nickel-filtered Cu Kα radiation. Powdered samples were analyzed by accumulating detector counts for 2.5 s at each diffraction angle in steps of 0.05° over the range $5° \leq 2\theta \leq 50°$.

Scanning electron microscopy, SEM, was carried out on a Phillips 505 instrument operated at 10 kV.

Results and Discussion

Properties of the Two Components. Representative DSC traces for the diacetylene-containing polyester, PE, and the poly[ethylene-*co*-(vinyl acetate)], EVA, are shown in Figure 1 for the materials both before and after molding. The data derived from the DSC traces are presented in Table 1.

Curves a and b of Figure 1 show that the melting endotherm of EVA is unaffected by processing and that the melting temperature, T_m, is 106 ± 2 °C, as located by the minimum in the curve. The most significant feature of the DSC trace for as-prepared PE, shown as curve c, is the very strong exotherm, peaking at 205 °C, due to topochemical cross-polymerization[10] of the diacetylene units in the backbone of PE. The change in structure on cross-polymerization is shown in Scheme 1.

PE is semicrystalline with a degree of crystallinity of 24% and a melting temperature of 119 °C.[10] (The melting endotherm is not evident in curve c of Figure 1 due to the low sensitivity used in order to observe the large exotherm but is detected at higher sensivities.[10]) Cross-polymerization can only occur when the spatial arrangement of the diacetylene units corresponds to lattice spacings which satisfy the criteria for topochemical polymerization.[13,14] Thus cross-polymerization oc-

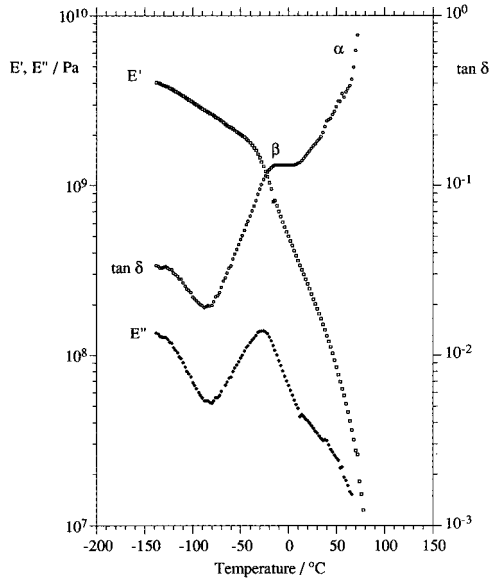

Figure 2. Plots of storage modulus (E'), loss modulus (E''), and loss tangent (tan δ) vs temperature for molded EVA.

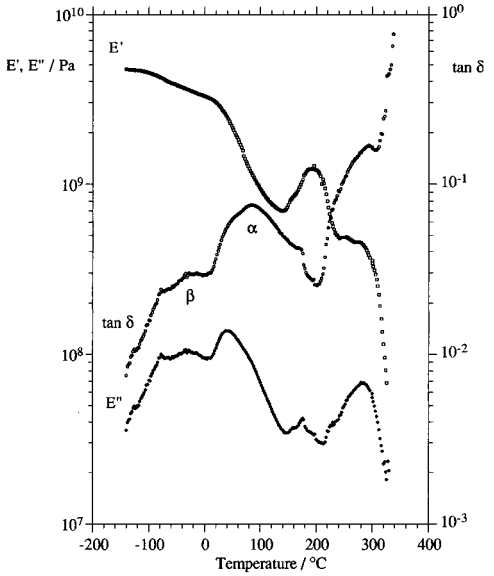

Figure 3. Plots of storage modulus (E'), loss modulus (E''), and loss tangent (tan δ) vs temperature for molded PE.

Table 2. DMA Data (1 Hz, 5 °C min^{-1}) for Molded Specimens of EVA, the Diacetylene-Containing Polyester, PE, and EVA/PE Blends

material	w_{PE}/%[a]	T_α^{PE}/°C[b]	T_β^{EVA}/°C[c]	E'/MPa[d]
EVA	0	*e*	−30	278 ± 10
PE	100	40[f]	*e*	3143 ± 36
B-20PE	20	*f*	−23	348 ± 19
B-40PE	40	*f*	−23	738 ± 29
B-60PE	60	*f*	−18	1155 ± 35
B-80PE	80	*e*	−18	1890 ± 70

[a] w_{PE} is the weight percentage content of PE. [b] T_α^{PE} is the peak value of temperature for the α-relaxation in molded PE from E'' vs temperature curves. [c] T_β^{EVA} is the peak value of temperature for the β-relaxation in EVA from E'' vs temperature curves. [d] E' is the value of the flexural storage modulus at 20 °C. [e] Peaks not observed. [f] Observed from E'' vs temperature curves as a peak for molded PE but only as shoulders between 10 and 90 °C for the blends.

curs in the crystalline regions of PE during molding[10] and the DSC trace for the resulting material (curve d of Figure 1) shows a much weaker cross-polymerization exotherm. The enthalpy of cross-polymerization, ΔH_{cp}^{PE}, is reduced by 84% from 652 to 102 J g^{-1} on molding. The exotherm observed in the region 300−360 °C is due to degradation and attempts to eliminate the residual cross-polymerization exotherm by molding either at higher temperatures or for longer periods resulted in degradation.[10] The molding conditions described in the Experimental Section were optimized to achieve the highest conversion of diactylene units commensurate with producing cross-polymerized PE that has a strong Raman spectrum.[10]

DMA of EVA shows (Figure 2 and Table 2) two relaxations in the temperature range −100 to +100 °C: the onset of the α-relaxation at about 80 °C correlates with the onset of melting observed by DSC (cf. Figure 1); the much weaker β-relaxation corresponds to that of polyethylene at about −25 °C which is due to local main-chain relaxation about branch points.[15] The modulus (280 MPa) of EVA at 20 °C is typical of medium density polyethylene.[16]

Figure 3 shows the DMA curves for molded PE which, through comparison with the DSC traces of PE shown in Figure 1, may be interpreted in terms of both chemical and physical processes. The peaks labeled α and β in Figure 3 are assigned to the glass transition and a secondary relaxation, respectively, on the basis of comparison with the relaxation behavior of poly(ethylene terephthalate) and poly(butylene terephthalate).[15] The E' curve reflects these assignments in that there is a small inflexion between −60 and −100 °C that is followed by a more significant decrease in E' corresponding to the glass transition of the amorphous phase. The reduction in E' at the glass transition from 3.0 GPa at 20 °C to 0.7 GPa at 140 °C is, however, less than expected given the relatively low degree of crytallinity (<30%). The arrest in the decrease of E' at 140 °C and the subsequent increase to a maximum of 1.2 GPa at 192 °C is consistent with the residual exotherm in the DSC trace of molded PE (curve d of Figure 1). These observations can be ascribed to the cross-polymerization of residual, active diacetylene units in the molded PE. Hence, the shoulder in tan δ and the small peak in E'' corresponding to the peak in E' do not identify physical relaxations but are physical manifestations of the chemical change which leads to increased cross-linking. The decrease in E' as temperature increases from 192 °C to about 240 °C may be ascribed to the continuation of the glass transition which has been shifted to higher temperature due to the additional cross-linking. There is a poorly-defined rubbery plateau between 240 and 280 °C prior to degradation leading to loss of structural integrity above 320 °C. The latter observation confirms the earlier interpretation of the peaks at 300−360 °C in the DSC traces of PE.

The WAXD pattern of EVA shown in Figure 4 is almost identical to that of medium density polyethylene[17] and shows two peaks located at 21.0 and 23.5°, an observation which indicates that EVA has a crystal structure similar to that of orthorhombic polyethylene.[17] The pattern for EVA is, however, distinguished by the presence of a shoulder on the left side of the major peak. Comparison of WAXD patterns a and b in Figure 4 shows that there is no effect on crystal structure due to processing conditions used during compression molding. This is consistent with the DSC traces of EVA, before and after molding (Figure 1), from which the enthalpy of fusion is seen to be unaffected (Table 1).

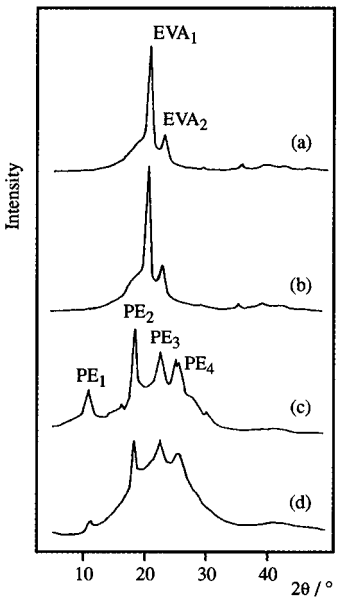

Figure 4. Wide-angle X-ray diffraction patterns of EVA (a) before and (b) after molding and of PE (c) as prepared and (d) after molding. The maxima in intensity labeled EVA_1 and EVA_2 and PE_{1-4} are Bragg reflections due to the crystalline regions in EVA and PE, respectively, and occur at ($2\theta \pm 0.2°$, $d \pm 0.01$ nm): EVA_1 (21.0°, 0.42 nm); EVA_2 (23.5°, 0.38 nm); PE_1 (11.6°, 0.76 nm); PE_2 (19.1°, 0.47 nm); PE_3 (23.3°, 0.38 nm); PE_4 (26.0°, 0.34 nm).

The WAXD pattern of the PE, as prepared, has been presented and discussed in detail previously.[10] This pattern is shown in Figure 4 as curve (c) together with the WAXD pattern, curve d, of molded PE for comparison. The locations of the four peaks labeled PE_1 to PE_4 are not significantly affected by molding with concurrent cross-polymerization, consistent with topochemical polymerization of active diacetylene units in the crystalline phase. There is, however, a clear effect of molding in increasing the size of the amorphous halo relative to the intensities of the crystal reflections (cf. Figure 4c,d). A possible explanation is that although cross-polymerization occurs in the solid state, not all of the diacetylene units in the crystalline phase are active and the inactive diacetylene units become disordered due to melting during molding. On cooling, only a proportion of the inactive diacetylene units return to the crystalline state, leading to a decrease in the degree of crystallinity and the observed enhancement of the amorphous halo.

DSC and WAXD Analysis of the Blends. In the preparation of the blends the two components, EVA and as-prepared PE, were first dissolved together and then coprecipitated. The effect of the dissolution/precipitation process on PE is to reduce the peak temperature for cross-polymerization from 205 to 186 °C and to reduce the enthalpy of cross-polymerization from 652 to 574 J g^{-1} (see Table 1). This implies that the perfection of the crystallites and the extent of crystallization are slightly reduced by this process, an inference that is consistent with the severe constraints on crystallization in the time scale of precipitation. Nevertheless, the blends obtained develop sufficient concentration of polydiacetylene cross-links during molding to facilitate studies of deformation micromechanics using Raman spectroscopy.[11]

The representative DSC traces of B-40PE shown in Figure 5 may be compared with those for the two components given in Figure 1. The significant features

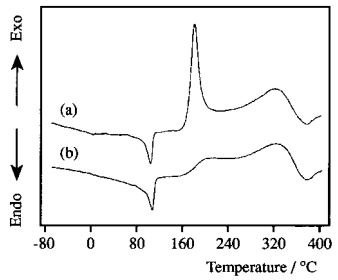

Figure 5. DSC traces of blend B-40PE (a) before and (b) after molding. (The sensitivity of the traces is constant.) Both traces show the melting endotherm of the EVA at ~100 °C. The cross-polymerization exotherm associated with the PE component has a maximum at 177 °C before molding and is considerably weaker after molding because cross-polymerization of PE has taken place.

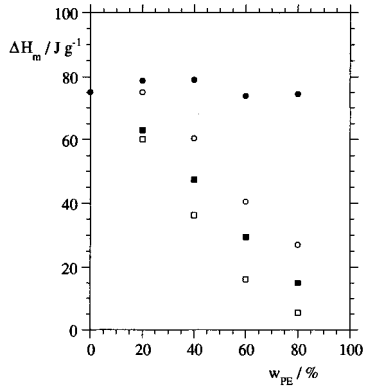

Figure 6. Variation of enthalpy of fusion, ΔH_m, of EVA with weight percentage of PE, w_{PE}, in the blends: enthalpy of fusion per unit mass of the blend, ΔH_m^B, before (■) and after (□) molding, and normalized to EVA content, ΔH_m^{EVA}, before (●) and after (○) molding.

of the traces for the blends before molding are the melting endotherm of EVA at about 100 °C and the very intense PE cross-polymerization exotherm with a maximum in the region 175−179 °C. After molding the EVA melting endotherm is still evident at about 100 °C, but only a weak residual exotherm is present showing that cross-polymerization has been effected.

Analysis of the DSC traces for the enthalpy of fusion, ΔH_m, of the EVA and for the enthalpy of cross-polymerization, ΔH_m, of the PE gives the data summarized in Table 1. In Figure 6, which shows the effect of blend composition upon the value of ΔH_m, there is an approximately linear decrease in ΔH_m with increasing PE content when ΔH_m is normalized to the total mass of blend. A better interpretation of the data is obtained by considering ΔH_m normalized to the EVA content of the blend (i.e., ΔH_m^{EVA}), which shows that within experimental variation, ΔH_m^{EVA} is independent of composition for the blends before molding. However, for the molded blends ΔH_m^{EVA} decreases substantially with increasing PE content, implying that during molding, crystallization of the EVA is inhibited by interaction with PE. Improved miscibility at the temperature of molding, changes due to cross-polymerization, and morphological changes may all contribute to this observation. In the precipitates obtained from the solution blending stage, the phase-separated EVA phase can anneal without significant limitation being imposed by the PE phase. During molding, miscibility between molten EVA and amorphous regions of PE can be

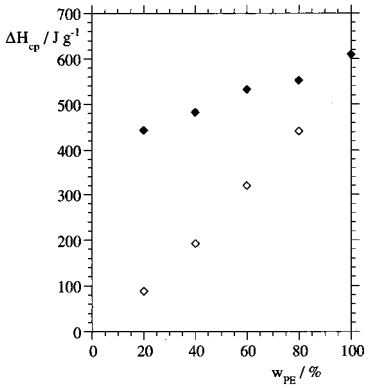

Figure 7. Variation of enthalpy of cross-polymerization, ΔH_{cp}, of PE with weight percentage of PE, w_{PE}, in the blends before molding: enthalpy of cross-polymerization per unit mass of the blend (◇), ΔH_{cp}^{B}, and normalized to PE content (◆), ΔH_{cp}^{PE}.

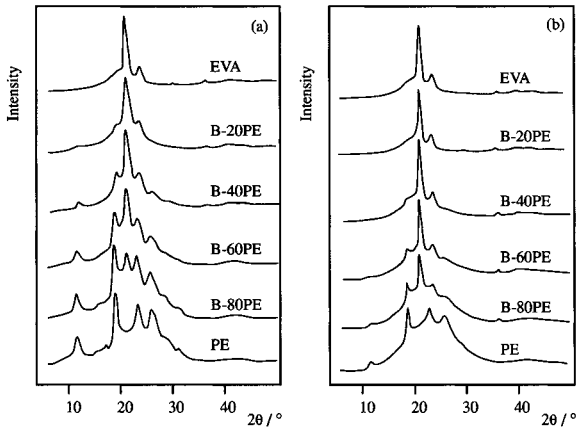

Figure 8. Wide-angle X-ray diffraction patterns of EVA, PE, and blends with different weight percentages of PE (given by the number in the code against each pattern): (a) before and (b) after molding.

expected to improve, leading to formation of molecular entanglements between the phases while the ordered regions of the PE phase simultaneously cross-link. EVA chains, entangled with chains of the cross-linked PE phase, will be restricted in their ability to undergo further crystallization, thus resulting in lower degrees of EVA crystallinity in the cooled moldings.

Figure 7 shows the variation with PE content of the enthalpy of cross-polymerization normalized to total mass of blend (ΔH_{cp}^{B}) and to the PE content of the blend (ΔH_{cp}^{PE}). It is clear that the enthalpy of cross-polymerization decreases as the EVA content of the blend increases, again indicating interaction between the two blend components during blending and/or molding.

The effects of molding upon the WAXD patterns for each of the materials is shown in Figure 8. Each blend shows the peaks from the two components with intensities approximately in proportion to blend composition. Additionally, the changes in the WAXD patterns after molding are in accord with the changes observed for the two components, as described earlier in this paper. The similarity in the spacings, defined by the peak positions in the WAXD patterns of the blends and of the EVA and PE, shows that blending has no obvious effect upon crystal structure.

Morphology of the Blends. In addition to the information provided by the DSC and WAXD experi-

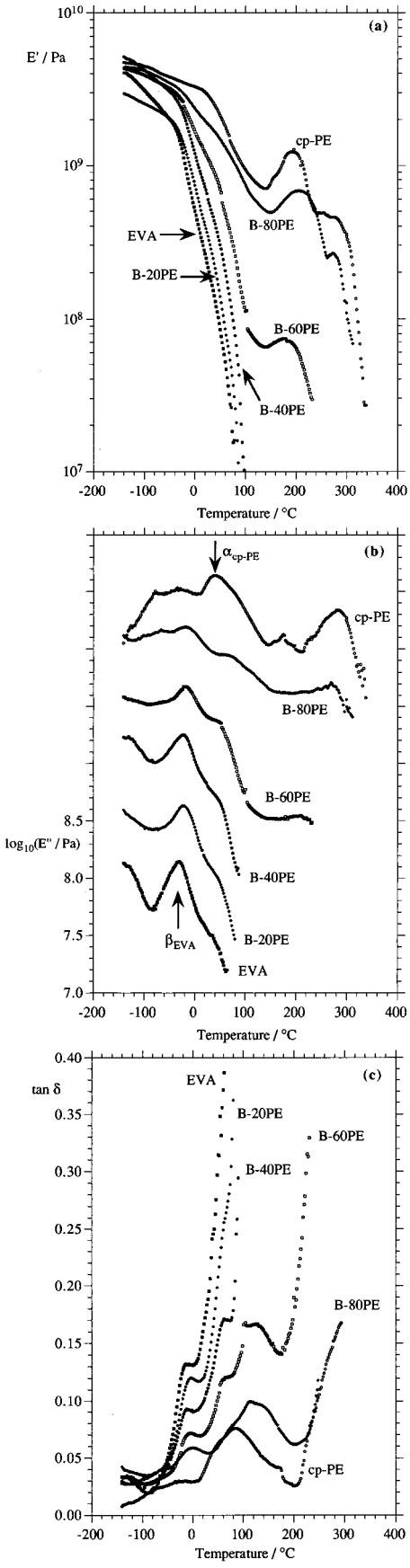

Figure 9. Plots of (a) storage modulus (E'), (b) loss modulus (E''), and (c) loss tangent (tan δ) vs temperature for molded EVA, cross-polymerized PE (cp-PE), and molded blends with different weight percentages of PE given by the number in the code against each curve. The E'' curves are offset by units of 0.5 $\log_{10}(E''/\text{Pa})$ for clarity.

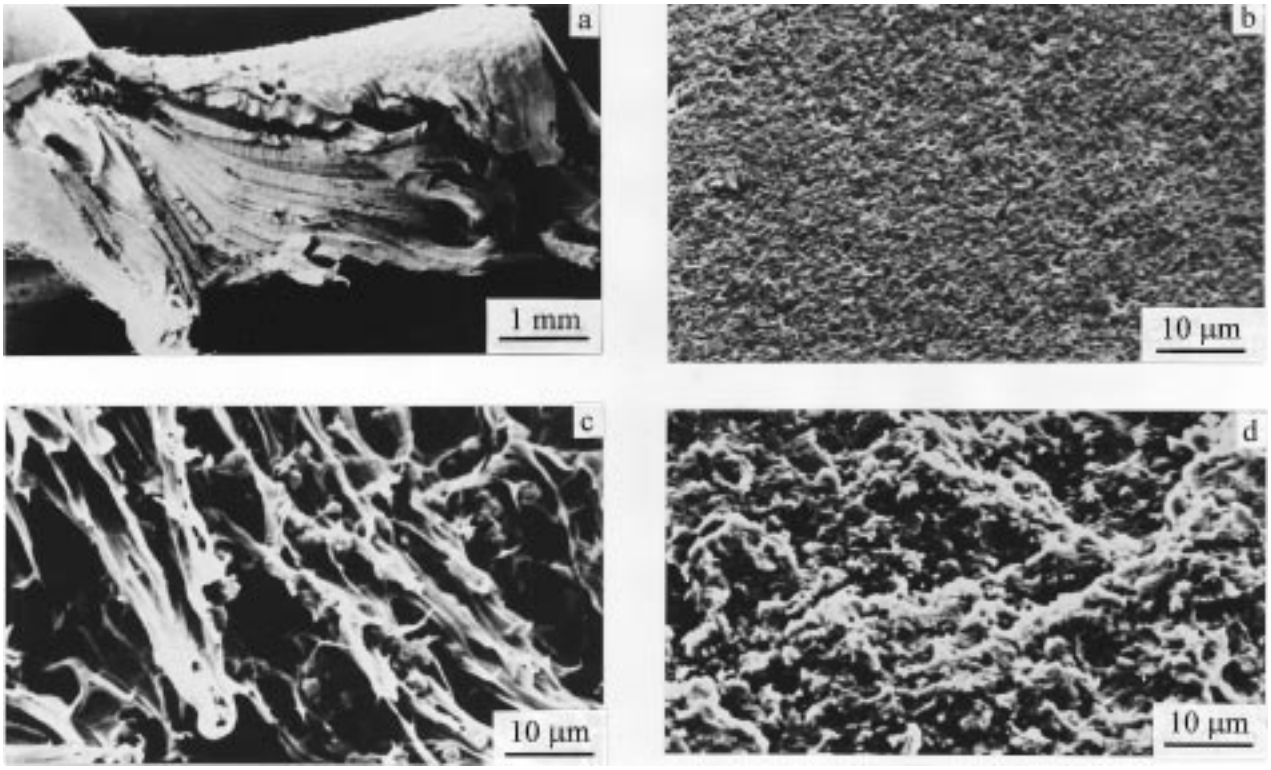

Figure 10. Representative SEM micrographs of tensile fracture surfaces of EVA (a), PE (b), B-20PE (c), and B-80PE (d).

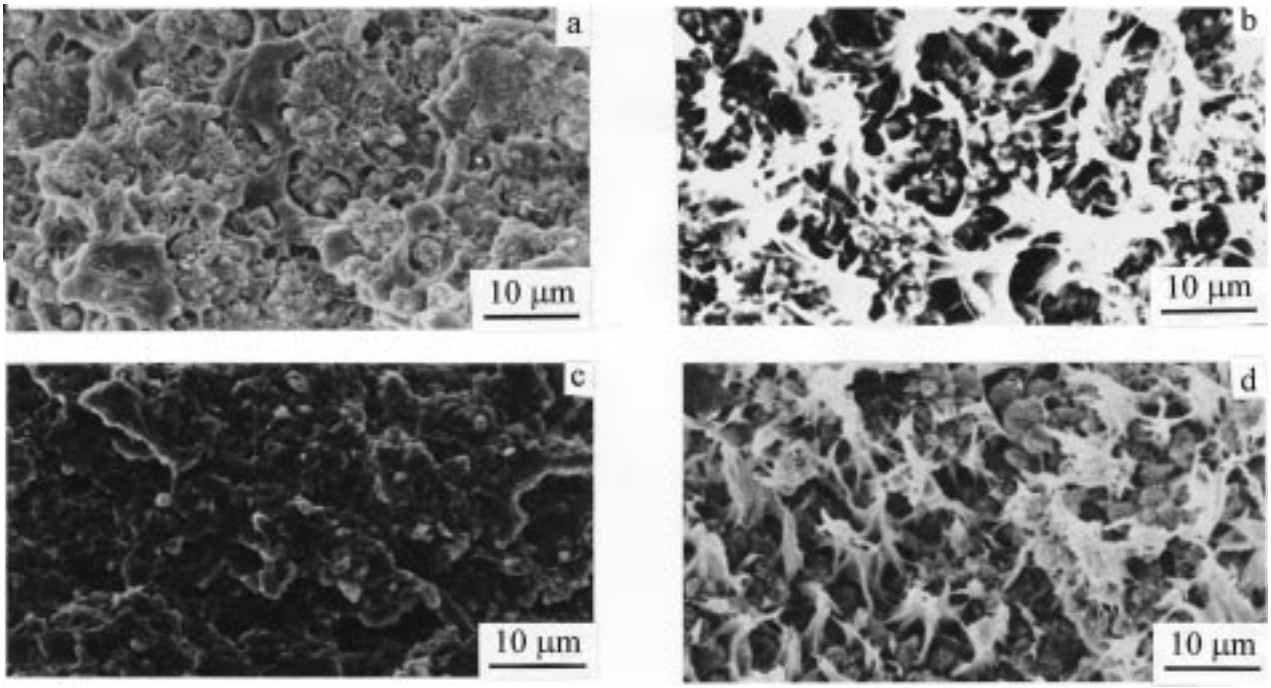

Figure 11. Representative SEM micrographs of regions of tensile fracture surfaces of B-40PE (a, brittle region; b, ductile region) and B-60PE (c, brittle region; d, ductile region). Inspection of the micrographs shows particles of cross-polymerized PE with sizes up to about 8 μm.

ments, the studies of deformation micromechanics described in the Introduction require a knowledge of blend morphology. The techniques that have been employed to examine morphology are DMA and SEM.

DMA curves for each of the molded blends and the two components are shown in Figure 9. The data derived from the curves are summarized in Table 2.

The storage moduli measured at 20 °C show a continuous increase as the PE content of the blend increases. The loss modulus curve for each blend shows the β-relaxation of EVA as a peak and the α-relaxation of cross-polymerized PE as a shoulder; the magnitude of E'' associated with each transition changes in accord with blend composition. The most significant change in dynamic mechanical behavior with PE content, however, is observed for blends B-20PE and B-40PE, which show a complete loss of mechanical integrity around 100 °C, a temperature well below that ($\sim$140 °C) at which further cross-polymerization and structural enhancement of the PE phase occurs. In contrast, the

B-60PE and B-80PE blends attain 140 °C without loss of mechanical integrity and show the associated increase in storage modulus. In relation to morphology, these observations indicate that the B-20PE and B-40PE blends have EVA as the continuous phase.

Representative SEM micrographs of tensile fracture surfaces of the two components and all the blends are shown in Figures 10 and 11. The fracture surface of EVA (Figure 10a) shows the extensive plastic deformation and yielding associated with the ductile failure of the material. In contrast, Figure 10b reveals a fine granular texture and an absence of plastic deformation on the fracture surface of cross-polymerized PE, which fails in a brittle manner. In the case of B-20PE (Figure 10c), drawn strands of EVA are clearly evident around regions of small irregular particles of cross-polymerized PE, indicating a continuous−discontinuous morphology with EVA as the continuous phase. The absence of drawn EVA on the fracture surface of B-80PE shown in Figure 10d when considered together with the brittle failure of the material suggests that the EVA is a dispersed phase in a cross-polymerized PE matrix. Across the composition range there is, therefore, a phase inversion which must be considered in the interpretation of the micrographs of the blends of intermediate composition, *viz.*, B-40PE and B-60PE. The fracture surfaces of both these materials show regions of ductile and brittle failure (Figure 11) and evidence of partial debonding of the particles of cross-polymerized PE, especially in the regions of ductile fracture, though the particles remain connected to the EVA by drawn fibrils of EVA. The micrographs for B-40PE indicate a continuous−discontinuous morphology similar to B-20PE, though the drawing of the EVA matrix around the particles of cross-polymerized PE in ductile regions is less extensive than for B-20PE (cf. Figures 10c and 11b). The morphology of B-60PE is less clear. The micrograph of the region of brittle fracture shows no distinct morphology, whereas that of the ductile region shows drawing of the EVA on a similar scale to that evident for B-40PE in Figure 11b, despite the expectation that cross-polymerized PE would form the continuous phase in B-60PE. This suggests that B-60PE has a co-continuous morphology.

In order to substantiate the inferences from the SEM micrographs, each of the molded blends was extracted with boiling toluene until the EVA was completely removed. Specimens of blends B-20PE and B-40PE collapsed into powders during extraction, an observation consistent with a continuous−discontinuous morphology in which EVA is the matrix. For B-60PE and B-80PE the specimens became friable but, more significantly, retained their shape and integrity confirming the presence of a continuous cross-polymerized PE phase, as shown by the SEM micrographs in Figure 12. There is, however, a distinct difference between the morphologies of the cross-polymerized PE phases in these two extracted blends. For B-80PE (Figure 12c) the morphology is clearly continuous−discontinuous. However, inspection of Figures 12a and 12b shows that for B-60PE the structure is much more open with what appear to be continuous open channels (left by the extracted EVA) similar in size to the continuous cross-polymerized PE phase. The conclusion to be drawn is that B-60PE has a co-continuous morphology.

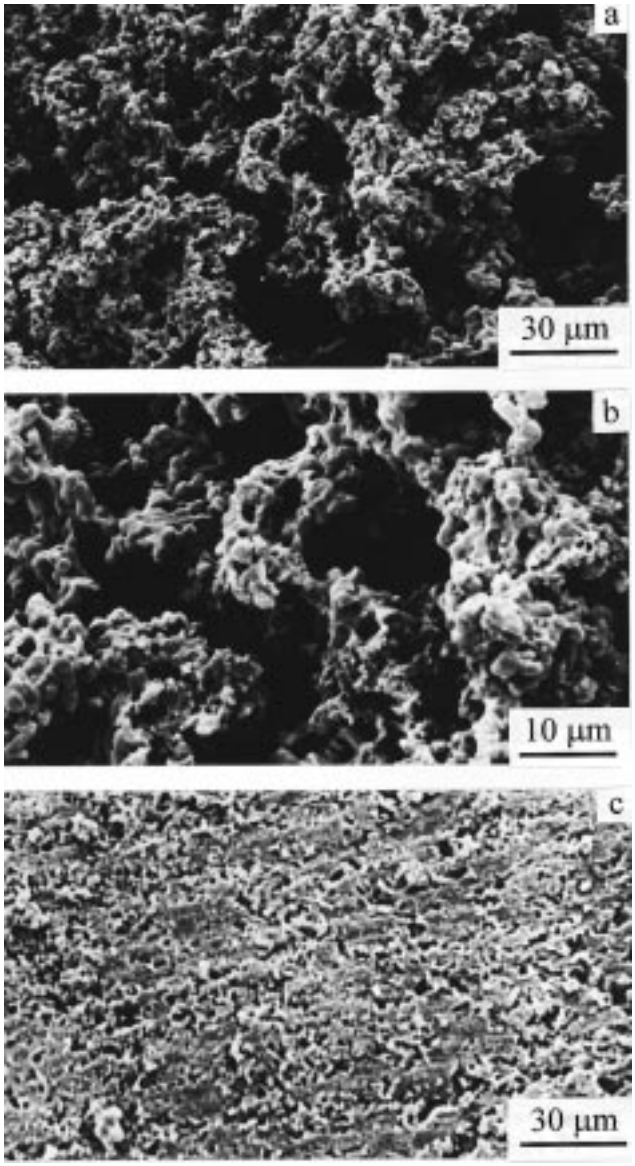

Figure 12. SEM micrographs of surfaces of solvent-extracted specimens of B-60PE (a and b) and B-80PE (c).

Conclusions

Blends of EVA and PE can be prepared without cross-polymerization of the PE by dissolution in a 50:50 tetrahydrofuran:toluene mixture at 80 °C, followed by coprecipitation into excess of 20:80 methanol:water mixture to yield cream-colored powders. Good moldings are obtained by compression molding under vacuum at 120 °C for 6 h with a 3 h warm-up period using a purpose-designed apparatus. During molding the blends show the color change from cream to deep purple that is characteristic of polymerization of diacetylenes.

Almost complete cross-polymerization is achieved during molding with only a small amount of reactive diacetylene units remaining, as shown by the relatively weak residual cross-polymerization exotherm (DSC) and small increase in modulus (DMA) in the temperature range 140−200 °C of the molded materials.

WAXD measurements show that the crystal structures of EVA and PE undergo no major change on molding. However, although T_m (≈106 °C) for EVA is not affected significantly by blending, ΔH_m^{EVA} decreases linearly with increasing PE content. The retention of

the crystal structure of PE during molding is consistent with topochemical cross-polymerization. The value of T_{cp} (175−179 °C) is essentially the same for each blend but the value of ΔH_{cp}^{PE} decreases linearly with increasing EVA content. The observed trends for variation of ΔH_{cp}^{EVA} and ΔH_{cp}^{PE} with composition indicate interactions between the two components that limit the extent of crystallinity in each phase.

SEM and solvent extraction experiments show that B-60PE has a co-continuous morphology, whereas the other blends have continuous−discontinuous morphologies.

The next paper[11] presents results from mechanical characterization and deformation micromechanics studies of the cross-polymerized blends in relation to composition and morphology. In particular, the paper reports use of Raman spectroscopy to determine quantitatively deformation in the cross-polymerized PE phase of the blends independent of overall blend deformation.

Acknowledgment. Financial support of the research work reported in this paper was kindly provided by Exxon Chemical. R.J.Y. is grateful to the Royal Society for support in the form of the Wolfson Research Professorship in Materials Science.

References and Notes

(1) Paul, D. R.; Newman, S., Eds., *Polymer Blends*; Academic Press: New York, 1978.
(2) Utracki, L. A. *Polymer Alloys and Blends*; Hanser: Munich, 1989.
(3) Folkes, M. J.; Hope, P. S. *Polymer Blends and Alloys*; Blackie: Glasgow, 1993.
(4) Day, R. J.; Stanford, J. L.; Young, R. J. *Polymer* **1991**, *32*, 1713.
(5) Day, R. J.; Hu, X.; Stanford, J. L.; Young, R. J. *Polym. Bull.* **1991**, *27*, 353.
(6) Hu, X.; Stanford, J. L.; Day, R. J.; Young, R. J. *Macromolecules* **1992**, *25*, 672, 684.
(7) Hu, X.; Stanford, J. L.; Day, R. J.; Young, R. J. *J. Mater. Sci.* **1992**, *27* 5958.
(8) Lovell, P. A.; Stanford, J. L.; Wang, Y.-F.; Young, R. J. *Macromolecules* 1992, Sept, preprints.
(9) Lovell, P. A.; Stanford, J. L.; Wang, Y.-F.; Young, R. J. *Polym. Bull.* **1993,** *30*, 347.
(10) Lovell, P. A.; Stanford, J. L.; Wang, Y.-F.; Young, R. J. *Polym. Int.* **1994,** *34*, 23.
(11) Lovell, P. A.; Stanford, J. L.; Wang, Y.-F.; Young, R. J. *Macromolecules* **1998**, *31*, 842.
(12) Wang, Y.-F. *Structure-Property Relationships in Model Diacetylene-Containing Polymer Blends*. Ph.D. Thesis, Victoria University of Manchester, 1992.
(13) Bloor, D. In *Developments in Crystalline Polymers-1*; Bassett, D. C., Ed.; Applied Science: London, 1982; p 151.
(14) Bloor, D. In *Quantum Chemistry of Polymers, Solid State Aspects*; Ladik, J., Andre, J. M., Seel, M., Eds.; D. Reidel: Dordrecht, 1984; p 191.
(15) McCrum, N. G.; Read, B. E.; Williams, G. *Anelastic and Dielectric Effects in Polymeric Solids*; John Wiley & Sons: London, 1967.
(16) Brandrup, J., Immergut, E. H., Eds. *Polymer Handbook*, 3rd ed.; John Wiley & Sons: New York, 1989; p V/23.
(17) Young, R. J.; Lovell, P. A. *Introduction to Polymers*, 2nd ed.; Chapman & Hall: London, 1991; p 266.

MA970071R